A Combined EPR and Quantum Chemical Approach to the Structure of Surface F_s^+(H) Centers on MgO

Elio Giamello* and Maria Cristina Paganini

Dipartimento di Chimica Inorganica, Chimica Fisica e Chimica dei Materiali, Università di Torino, Via P. Giuria 9, 10125 Torino, Italy

Damien M. Murphy

Department of Chemistry, University of Wales Cardiff, 50 Park Place, P. O. Box 912, Cardiff CF1 3TB, U.K.

Anna Maria Ferrari and Gianfranco Pacchioni

Dipartimento di Chimica Inorganica, Metallorganica e Analitica, Università di Milano, Via Venezian 21, 20133 Milano, Italy

Received: August 23, 1996; In Final Form: November 3, 1996[⊗]

F_s^+(H) color centers at the surface of MgO have been studied using a combined EPR and quantum chemical approach. F_s^+(H) are paramagnetic excess electrons centers where the unpaired electron is trapped in a surface anion vacancy. They are formed at the surface of thoroughly dehydrated MgO (1073K) upon UV irradiation under hydrogen in parallel with the formation of minor fractions of different color centers. The whole EPR spectrum resulting from irradiation has been analyzed by simulation of the experimental profile. F_s^+(H) centers are characterized by an axial **g** tensor and display a hyperfine interaction with a hydrogen nucleus (belonging to an hydroxyl group stabilized nearby the vacancy) and two distinct families of ^{25}Mg nuclei characterized by a large (10.5 G) and a small (0.7 G) hyperfine coupling constant, respectively. Both EPR and ab initio calculations on clusters of ions converge in indicating that the features of the centers are due to the polarization of the electron density by the positive charge of the hydrogen in the OH group toward two (or possibly three) equivalent magnesium ions of the vacancy close to the OH group itself. The formation mechanism of the centers is strictly analogous to that occurring upon contact of low ionization energy metals with the surface of MgO leading to the formation of another type of color centers. Partially hydrated MgO samples also give rise to another family of paramagnetic center based on electrons trapped in anion vacancies. This finding indicates that the structure of the partially hydroxylated oxide and the mechanism of its dehydration are still open questions.

Introduction

The study of bulk point defects in ionic crystals (mainly alkali halides and alkali-earth oxides) has been quite comprehensive over the past 40 years.[1−4] Among the many types of point defects investigated in detail, the bulk V centers (electron deficient centers) and bulk F centers (excess electron centers) have attracted the most attention. In the former case the center is formed by removal of an electron from an anion leaving a *hole*, whereas in the latter case the center (also called *color center*) is formed by trapping an electron at an anion *vacancy*.

On the other hand extensive research on the nature of the surface counterparts to these point defects has been rather limited in the past.[5−10] In the particular case of the F_s type centers (the s subscripts indicates a surface center), recent efforts have begun to reveal the interesting nature and properties of the surface centers.[11−13] One reason for this growing interest arises from the lower symmetry and coordination of the surface center compared to the bulk center as manifested in the magnetic properties. Another reason of interest is related to the interactions taking place between the surface trapped electrons and molecules of an external gaseous or liquid phase adsorbed on the surface.[14−16] These interactions can in some cases initiate an intriguing chemical reactivity involving electron transfer from the solid to adsorbed molecules and offer new insights into the early stages in the activation of small molecules.[17−19]

The two types of surface color centers which can in principle be localized on the surface of the alkali-earth oxides are the F_s and F_s^+ centers.[13] The F_s^+ center holds a single electron in the surface anion vacancy (the anion vacancy itself is sometimes labeled F_s^{2+}), whereas the F_s center contains two trapped electrons in the F_s^{2+} vacancy. Both F_s and F_s^+ centers are responsible for the blue-violet color of the samples, but only the F_s^+ centers, which contain a single unpaired electron, are paramagnetic and therefore detectable by EPR spectroscopy.

In the case of the alkali-earth oxides four basic methods can be adopted to generate color centers localized *at the surface* of the crystals. These methods include UV irradiation in the presence of adsorbed H_2 or D_2,[6−10] exposure of the oxide to H atoms (generated in an electrical discharge through H_2 gas),[20] γ irradiation,[3−5] and addition of low ionization energy metals.[11−13,19,21,22]

Using the latter two procedures, surface F_s and F_s^+ centers are generated.[13] In the former two cases, UV irradiation in the presence of H_2 or exposure of the oxide to H atoms created in an electrical discharge, generates surface F_s^+(H) centers.[8,13,20] These can be regarded simply as F_s^+ color centers but are characterized by a distinctive superhyperfine interaction between the trapped electron and a proton likely belonging to a nearby hydroxyl group; hence the label F_s^+(H). Most of our current

* Author for correspondence.
[⊗] Abstract published in *Advance ACS Abstracts,* January 1, 1997.

S1089-5647(96)02619-3 CCC: $14.00

knowledge about these F_s^+(H) centers is based on the interpretation of experimental data obtained some years ago by Tench and co-workers.[6−10] A detailed formation mechanism of these centers, generated by UV irradiation of MgO in a hydrogen atmosphere, and the origin of the hydroxyl group which interacts with the unpaired electron was never explicitly accounted for. The structural model proposed to account for the nature of F_s^+-(H), on the basis of available EPR data, was described as an electron trapped in a surface anion vacancy on the (001) plane of MgO and interacting with a nearby OH^- group.[8] However this model should now be reexamined based on recent advances in our understanding of the surface chemistry and morphology of MgO, new and more detailed EPR data on the F_s^+(H) centers and recent developments in quantum mechanical calculations.

MgO, in fact, has lately become the object of several theoretical investigations as a model oxide surface for calculations by quantum mechanical methods.[23−28] This is mainly due to the simple structure of the oxide (NaCl structure), its high ionicity, and the small atomic number of the constituent elements, Mg and O. All these factors converge in supporting MgO as a particularly attractive model system for ionic oxides, thereby allowing the application of highly sophisticated computational techniques. In the present work the quantum mechanical calculations were performed, by means of cluster models and ab initio wave functions, to evaluate the energy and the electron distribution for various possible structural models of the surface color centers.

Under the experimental point of view, MgO also offers significant advantages over other oxides. It is a well-characterized crystalline ionic insulator, it can be prepared in a high purity form or doped with selected extrinsic impurities, and by careful choice of the preparation method it can be prepared with a wide range of high surface areas. This consequently increases the probability of generating sufficient concentrations of surface centers for easy spectroscopic detection. Several experimental techniques have now clearly evidenced the homogeneous size and regular shape of the small cubic crystallites of the oxide despite the polycrystalline nature of the high surface area material.[29−32] Spectroscopic investigations have also clearly pointed out the role of the different coordination sites (5C, 4C, or 3C) present on the surface and of the abundant morphological defects such as edges, steps, kinks and terraces in the overall surface chemistry of MgO.[30,33,34] In fact the combined utilization of theoretical calculations and experimental investigations is now rapidly advancing to a level of sophistication whereby surface structure, features of surface defects and adsorbed species, and even the understanding of a complex phenomenon like surface reactivity can be described with surprising accuracy.

The aim of the present paper is to revisit the problem of F_s^+-(H) formation and structure and therefore provide new evidence on the nature of the center itself. Although the old model of Tench[8] has some valid points in the basic assumptions concerning the nature of the center and the origin of H superhyperfine interaction, the new evidence reported here (based on the current EPR experimental data, careful computer simulation of the EPR spectra, and comparison of these experimental results with quantum mechanical calculations) allow new insights into unresolved problems such as the conditions for the formation of the centers, the magnitude, and the origin of the ^{25}Mg hyperfine structure and its relationships with the presence of an hydroxyl group interacting with the electron.

Experimental Section

High-purity MgO (Johnson Matthey) was hydroxylated to the corresponding hydroxide, $Mg(OH)_2$, by overnight treatment in water at 350 K, and finally dried in air. To produce high surface area (HSA) MgO, the magnesium hydroxide powder was slowly decomposed for ∼16 h under a dynamic $10^{-4}-10^{-5}$ Torr vacuum at 523 K.[12] The HSA MgO oxide was then activated under vacuum at 1073 K (i.e., $T_{dehy} = 1073$ K) for 1 h, obtaining a completely dehydrated material. The surface area of the activated oxide was ∼170−200 m^2/g.[12]

F_s^+(H) or F_s^+(D) centers were generated on the surface of the dehydrated MgO as follows. Hydrogen or deuterium (∼100 Torr) was added to the sample at 298 K, and the powder cooled to 77 K by placing the EPR cell in liquid nitrogen. The sample was then exposed to a UV low-pressure mercury vapor lamp for about 1 h, with occasional mixing of the contents in order to expose fresh MgO to the lamp. The excess H_2 or D_2 was then evacuated at 298 K from the now blue sample prior to EPR spectra recording. In a separate experiment, the above procedure was also repeated on two samples of partially hydroxylated MgO which had been dehydrated, as described above, but at lower temperatures ($T_{dehy} = 773$ and 873 K).

The high-temperature activated oxide ($T_{dehy} = 1073$ K) was also exposed to γ-rays at a dosage of 2 Mrad and at temperatures of ca. 313 K. This produces the surface F_s^+ centers as described elsewhere.[4,9,13]

X-band CW-EPR spectra were recorded at 298 K on a Varian E-109 spectrometer equipped with a dual cavity or, alternatively, on a Bruker ESP 300E series spectrometer. This temperature was used because at 77 K the spectra of color centers are noisier compared to those recorded at 298 K. This is probably due to the increase of cavity perturbation induced by the presence of the large amount of trapped electrons.

The Varian EPR spectrometer was connected to a CS-EPR Stelar data station, allowing spectra recording and careful double integration of the signals. Varian pitch ($g = 2.0028$) was used in this case for g value calibration. The EPR computer simulations were obtained using a program for a personal computer derived by the SIM14S program (QCPE 265). Optimization routines based on the simplex minimization procedure were adopted to refine the simulation.[35]

Results

EPR Spectra. After UV irradiation in the presence of H_2 or D_2, the MgO ($T_{dehy} = 1073$ K) powder develops a pale blue color and the parallel formation of the EPR spectra shown in Figure 1a,b, respectively. The EPR spectra are due to the simultaneous presence of at least three distinct paramagnetic species (labeled centers A, B, and C), and these spectra are normally quite reproducible. Only the relative intensity of the various species present (A, B, or C) varies slightly from one experiment to the next.

Main Features of the EPR Spectra. Figure 1a is dominated by a species which resonates close to the free-electron value and which has axial symmetry and a characteristic doublet hyperfine structure (with a coupling constant of about 2 G) due to the interaction with a proton. This species, labeled as center A in Figure 1a, has been previously reported in the past[6,8,10,13] and assigned to the surface F_s^+(H) center. The doublet structure in Figure 1a is transformed into an unresolved triplet in Figure 1b with a smaller coupling constant of about 0.3 G as expected when D_2 ($I = 1$) is used instead of H_2 ($I = {}^1/_2$). A second species, labeled center B, is also visible in Figure 1a. This second center does not have a doublet hyperfine structure (as confirmed by the computer simulation discussed in the next section) and so does not interact (or has only a negible interaction) with a proton. The third species responsible for the weak signal at low field in Figure 1a is labeled center C.

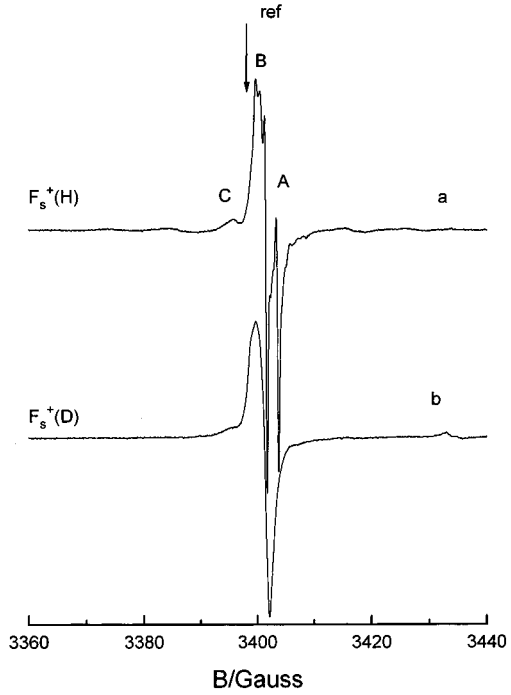

Figure 1. EPR spectra of the color centers on the surface of MgO after UV irradiation under hydrogen (a) and deuterium (b).

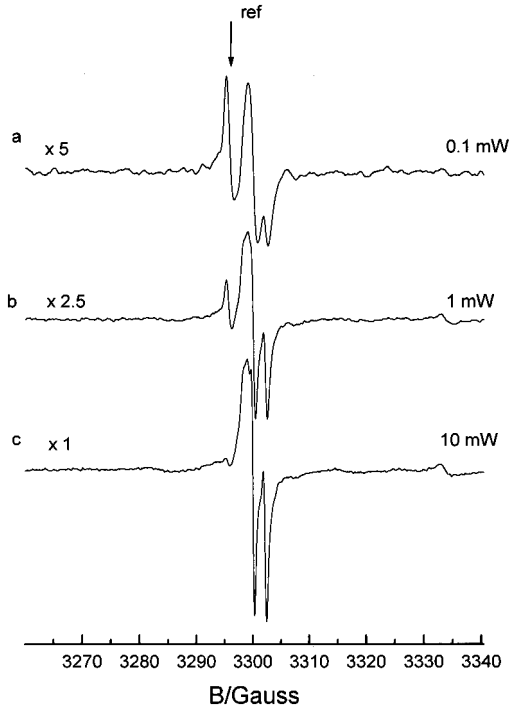

Figure 2. Spectrum in Figure 1 recorded at three different microwave power levels.

This signal is clearly not an associated component of centers A or B since it has a characteristically different saturation profile. The distinct saturation behaviour of center C compared to centers A and B is clearly evidenced in Figure 2, after the EPR spectra were recorded at different microwave powers.

The EPR spectra of the γ-irradiated MgO oxide is shown in Figure 3a. The computer simulation of the experimental spectrum is also shown in Figure 3b for comparison. The spectrum in Figure 3a appears to be built up by the minor contributions from center E (the low-field component) and traces of center A (present due to some residual OH groups which were not eliminated by thermovacuum treatment) as indicated by the weak high-field line. However Figure 3a is dominated

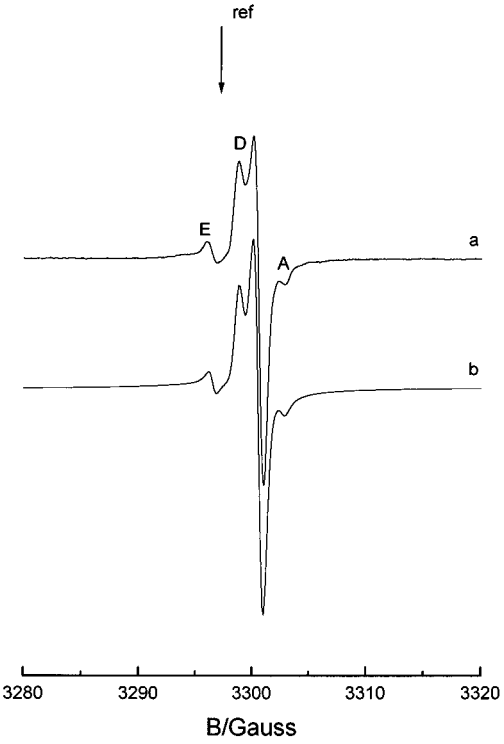

Figure 3. Experimental (a) and computer simulated (b) spectra of the color centers on the surface of MgO after γ-irradiation.

by another paramagnetic species labeled center D. Center D is an axial species specific to the γ-irradiated samples and can be assigned to a surface F_s^+ color center.[3−5]

Except for species C (whose features will be detailed in the following), all of these paramagnetic species on MgO (centers A, B, D in Figures 1−3) are essentially surface species. This is deduced by the fact that the **g** tensor of the species are anisotropic, as expected for surface color centers. Furthermore the blue color of the sample is immediately bleached by adsorption of various gaseous molecules such O_2, CO, and CO_2. The signals in Figures 1−3 are then immediately destroyed with the subsequent formation of the corresponding radical anions O_2^-, CO^-, and CO_2^- on the MgO surface as evidenced by EPR[16−19] and rationalized by recent ab initio calculations.[36]

A sextet hyperfine structure with about a 10 G coupling can be seen in the outer parts of Figure 1a,b. This sextet (whose lines are broader than those of the main signal) is clearly due to the interaction of the trapped electron with ^{25}Mg ($I = {}^5/_2$, 10.13% natural abundance), since ^{25}Mg is the only nucleus present in the system with a magnetic moment of $^5/_2$. On the basis of the intensity and as evidenced below by computer simulations, the sextet is related to the most abundant center A in Figure 1. Minor features can also be detected as superimposed weak lines on the main doublet structure. As discussed later, these lines arise from a weaker hyperfine interaction with the ^{25}Mg nucleus.

The outer wings of Figures 1a,b and 3 are shown in overamplified form in Figure 4a−c, respectively. It can be easily seen that the sextet structure of ∼10 G due to ^{25}Mg is clearly visible on the samples containing F_s^+(H) and F_s^+(D) centers (Figure 4a,b); the sextets have different relative intensities due to the different concentrations of F_s^+(H) and F_s^+(D) centers present in the two distinct MgO samples. However, the sextet is clearly absent in the spectrum of the γ-irradiated MgO (Figure 4c). The surface F_s^+ color centers responsible for species D should also in principle interact with ^{25}Mg nuclei since in all F color centers the unpaired electron is trapped in an anion vacancy. The absence of the sextet in Figure 4c

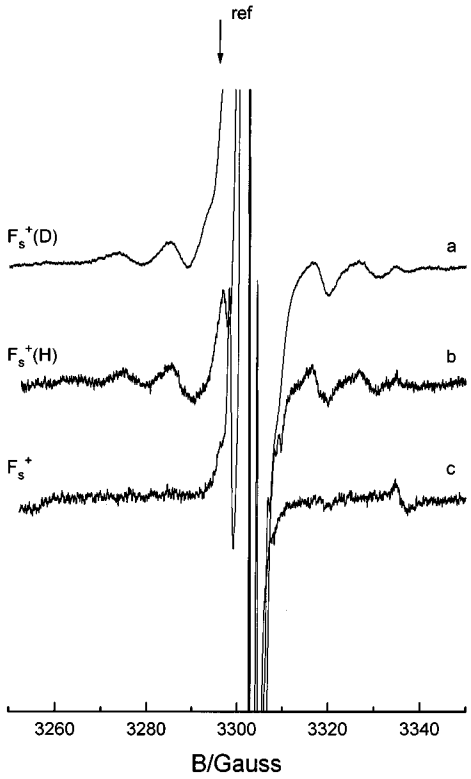

Figure 4. Comparison of the overamplified profiles of the wings of the spectra in Figures 1b,a and 3a (a, b, c, respectively).

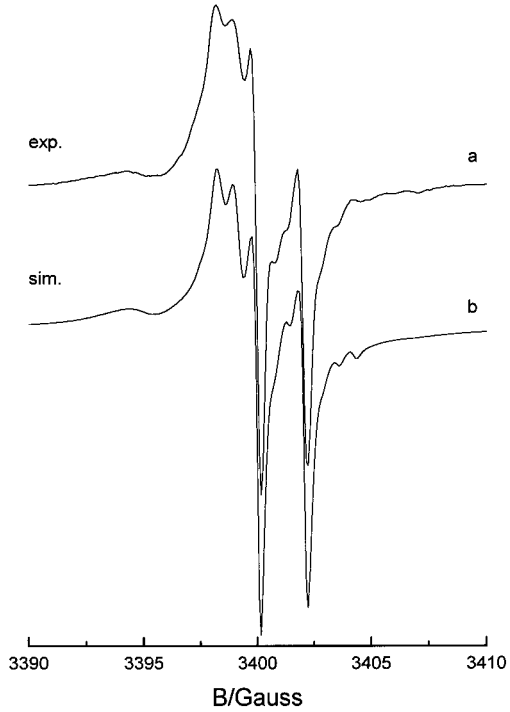

Figure 5. Computer simulation of the central portion of the spectrum in Figure 1a (UV irradiation under H_2).

indicates at least that the distribution of electron density in the two types of centers (A and D) is different from one case to the other. No evidence of a larger sextet at 25 G as proposed some years ago by Tench and co-workers[5,8] was ever found in the current work. This suggests a possible interference of some impurity (Mn^{2+}) in their experiments.

Simulation of EPR Spectra. Figure 5 shows the central part of the spectrum from Figure 1a as generated on UV-irradiated MgO in H_2 (Figure 5a), together with the computer simulation (Figure 5b). The simulation has been performed by assuming the simultaneous presence of three different species (corresponding to the centers labeled A−C in Figure 1). The computer simulation of the γ-irradiated sample is also shown in Figure 3b. The spin Hamiltonian parameters used in the two simulations are listed in Table 1. The simulation of the spectrum in Figure 1a is not an easy task as the experimental spectrum is the result of the overlap of the signals of at least three distinct species. The spectral parameters of the various species have been initially obtained by visual comparison between the experimental spectrum and its simulation. In a successive step they have been optimized by means of a simulation routine based on the Simplex method. In principle, it is possible that a somewhat different set of parameters could equally well account for the experimental spectrum profile. The errors affecting the various parameters are therefore also indicated in Table 1. The reported values correspond to the changes that are required to cause clearly appreciable modifications in the simulated spectrum.

Center A was found to be the most intense and the most complex in the simulation of the experimental spectrum. As center A is the only one of the three species on the MgO sample which exhibits coupling with a H nucleus, it can be indicated as the true F_s^+(H) center and represent the majority (72%) of all the observed species on MgO obtained by UV irradiation under hydrogen. This center has an axial **g** tensor with $g_{\|} = 2.0007$ and $g_{\perp} = 1.9996$ and is characterized by a hyperfine coupling with H ($A(^1H)$) and also by two separate sextets due to the interaction with two inequivalent ^{25}Mg cations (labeled $A(^{25}Mg)_1$ and $A(^{25}Mg)_2$, respectively); see Table 1. The interaction with H results in an axial hyperfine tensor with the larger value (2.07G) centered on $g_{\perp}$ and the smaller 0.4 G coupling on $g_{\|}$. The two different couplings with ^{25}Mg are both characterized by slightly axial tensors; the larger coupling ($A(^{25}Mg)_2$, $A_{\|} = 11.4$ G, $A_{\perp} = 10.5$ G) is responsible for the broad hyperfine lines visible (Figure 5) in the outer parts of the spectrum, while the smaller one ($A(^{25}Mg)_1$, $A_{\|} = 0.75$ G, $A_{\perp} = 0.73$ G) is responsible for the weak lines present in the inner parts of the spectrum. At the present state of elaboration of a model for the centers, the axes of the various tensors are assumed to be coincident. The smaller hyperfine coupling has never been reported before, and it is observed in the present work because of the relatively good resolution of the spectra. The line width of the external wings is quite large in comparison with that of the corresponding central signal because of heterogeneous broadening effects caused by the simultaneous presence of ^1H, $(^{25}Mg)_1$ and $(^{25}Mg)_2$ hyperfine interactions, by the anisotropy of both **g** and **A** tensors and by the normal effects of structural heterogeneity which are always found in polycrystalline solids. All these effects have been taken into account in the simulation using a line width, for the ^{25}Mg hyperfine structure, about three times larger than that of the central portion of the spectrum.

The natural abundance of ^{25}Mg is 10.13% so that the relative amounts of F_s^+(H) sites coupled to give either a large sextet, $A(^{25}Mg)_2$, or a small sextet, $A(^{25}Mg)_1$, must be calculated on the basis of some hypothesis on the structure of the defect center. The results of our simulation study of the Mg hyperfine structures are summarized in Figure 6, and the adopted approach is illustrated in the following. All of the *A* centers (i.e., the F_s^+(H) species) are coupled to a proton. But the relative number of F_s^+(H) centers displaying the preferential and large $A(^{25}Mg)_2$ interaction should be only 10.13% if this interaction was, as indicated by Tench,[8] with *one* particular ^{25}Mg cation. Computer simulation of this large sextet based on a 10.13% intensity probability does not however satisfactorily account for the observed intensity of the large experimental hyperfine structure ($A(^{25}Mg)_2$, Figure 6a). In this case a more complicated

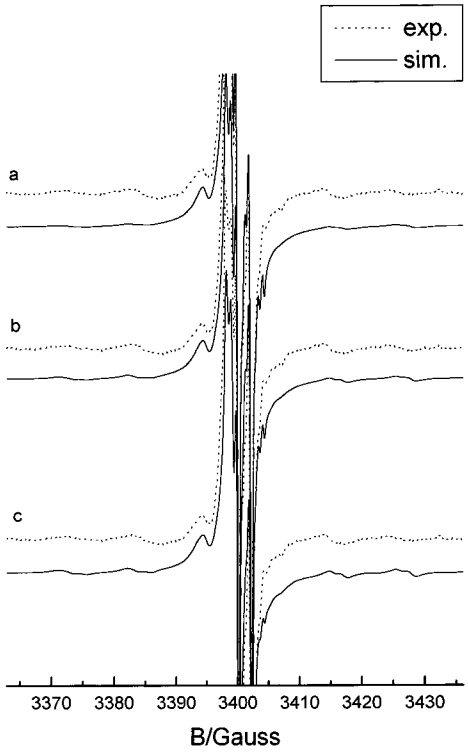

Figure 6. Comparison of the EPR simulations of the external wings of the spectrum of F_s^+(H) centers (Figures 1a and 4a). The three profiles have been obtained by hypothesizing the presence of 1, 2, and 3 magnetically equivalent Mg^{2+} ions on a total number of four cations in the vacancy (see text).

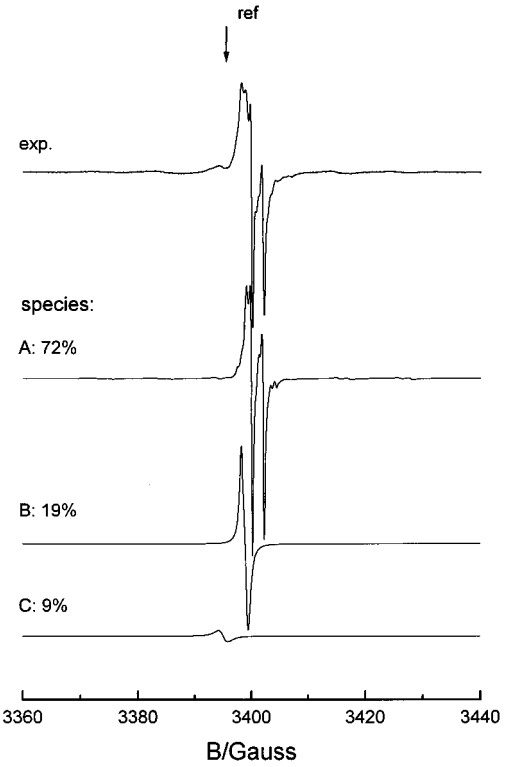

Figure 7. Simulated profiles of the three species composing the experimental signal obtained upon UV irradiation under H_2. The figures on the left-hand side indicate the relative abundance of the species.

distribution of equivalent Mg cations must be considered as being responsible for the sextet. The next alternative distributions are those considering that the large sextet arises from the interaction of the electron with *more than one* equivalent Mg^{2+} cation. The probability of finding m $^{25}Mg^{2+}$ nuclei in a given array of n equivalent Mg^{2+} ions can be calculated using the following formula:

$$P_n(m) = \binom{n}{m} p^{n-m} q^m \qquad (1)$$

where q is the natural abundance of ^{25}Mg (0.1013), p is $(1 - q)$, and $\binom{n}{m}$ the binomial coefficient. The spectra reported in Figure 6a−c have been calculated for $n = 1$, 2, and 3 respectively. Furthermore, to estimate the contribution to the smaller $(^{25}Mg)_1$ hyperfine, we assumed $N = 4$, N being the total number of Mg^{2+} cations surrounding the vacancy. Hence the number of $(^{25}Mg)_1$ cations with small hyperfine constant (supposed equivalent) is $(N - n)$.

The probability of having one $^{25}Mg^{2+}$ cation ($m = 1$) in a pair ($n = 2$) of equivalent ions is about 18% which rises to 24% if $n = 3$. The corresponding probability of having two ^{25}Mg in these two arrays is low (1% and 2.7%, respectively) and negligible in terms of contribution to the spectral line intensity. The two latter cases in Figure 6 more satisfactorily account for the observed intensity. The changes in the spectra passing from a 4 Mg^{2+} vacancy to a 5 Mg^{2+} vacancy ($N = 5$) are unappreciable. The simulation study thus suggest that the unpaired electron preferentially interacts with more than one Mg^{2+} ions but does not allow the exact determination of the total number of ions surrounding the vacancy. The two (or three) $(Mg^{2+})_2$ ions have been assumed equivalent in the simulation, but a moderate degree of nonequivalency is also compatible with the spectral profile due to its large line width.

Center B represents 19% of all the species present in the spectrum of UV-irradiated MgO (Table 1). It is an axial signal (Table 1) with similar $g_{\|}$ and $g_{\perp}$ values but no hyperfine interaction with a proton and, very likely, with ^{25}Mg. The g values and the general saturation behavior of signal B suggest that this species is also a surface F_s^+ center.

Center C represents only a minority of all the paramagnetic centers present on the sample. For the spectrum reported in Figures 1a and 5a, recorded at 10 mW microwave power, about 9% of all species present are due to center C. This value is however purely formal since, as shown by Figure 2, at this microwave power the species is nearly saturated.

The result of the above spectral simulation is, considering the complexity of the problem, quite satisfactory in that all of the main features in the experimental spectrum are adequately accounted for using physically meaningful data. To better illustrate the individual signals present (related to centers A, B, and C) which collectively account for the entire spectrum, Figure 7 compares these three signals (uniquely derived by the simulation described above) with the experimental spectrum.

TABLE 1: Spin Hamiltonian Parameters of F_s^+(H) and F_s^+ Centers

		abs	g			A(H)		$A(^{25}Mg)_1$		$A(^{25}Mg)_2$	
	species	%	$\|\|$	$\perp$	iso	$\|\|$	$\perp$	$\|\|$	$\perp$	$\|\|$	$\perp$
UV under	A	72	2.0007 ± 0.0002	1.9996 ± 0.0002		0.4 ± 0.1	2.07 ± 0.02	0.75 ± 0.03	0.73 ± 0.03	11.4 ± 0.1	10.5 ± 0.1
H_2	B	19	2.0013 ± 0.0002	2.0007 ± 0.0002		−	−	unresol		unresol	
	C	9			2.0032 ± 0.0002	−	−	unresol		unresol	
γ-irr	D	70	2.0015 ± 0.0002	2.0003 ± 0.0002		−	−	unresol		unresol	
	A	25	2.0007 ± 0.0002	1.9996 ± 0.0002		0.4 ± 0.1	2.07 ± 0.02	unresol		unresol	
	E	5			2.0029 ± 0.0002	−	−	unresol		unresol	

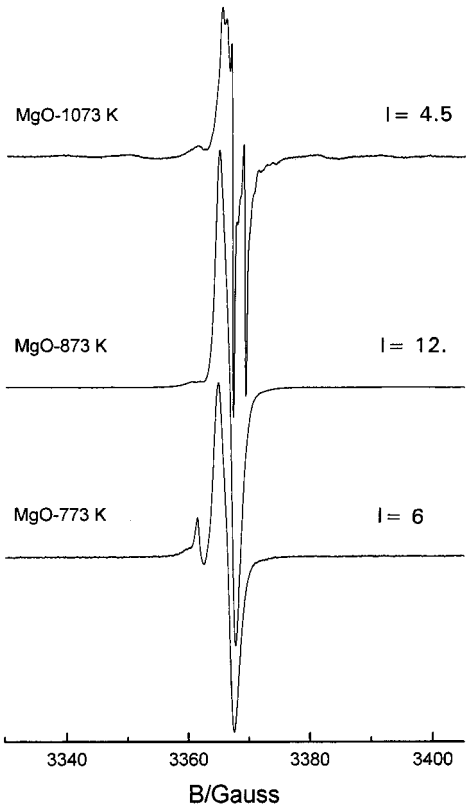

Figure 8. Experimental spectra obtained upon irradiation under hydrogen of samples dehydrated at different temperatures. The figures on the right-hand side represent the intensity of each spectrum in arbitrary units.

Spectra of Variously Dehydrated Samples. To monitor the effect of the extent of surface hydration on the formation of F_s^+(H) centers, UV irradiation under H_2 has been performed on three samples of equal weight but dehydrated at 773, 873, and 1073 K, respectively. The resulting EPR spectra are shown in Figure 8. On the right-hand side of each spectrum the relative intensities (in arbitrary units) of each spectrum are indicated. Three important facts show up from this experiment:

(a) In all three cases electron trapping centers are formed as indicated by the pale blue color of the materials and by the instantaneous reaction of electron transfer toward oxygen to give adsorbed superoxide ions (O_2^-).

(b) The highest number of centers is observed for MgO outgassed at 873 K.

(c) The two spectra in Figure 8b,c are not due to F_s^+(H) centers. This is indicated by their *g* values (which are slightly different from those of center A) and by the absence of any ^{1}H and ^{25}Mg hyperfine structure. The F_s^+(H) centers described above are found only on the sample dehydrated at 1073 (Figure 8a).

The above results indicate that oxygen vacancies are also formed upon partial dehydration of the hydroxylated MgO at temperatures lower than 1073 K. These oxygen vacancies, however, are clearly capable of electron trapping but give rise to centers different from those observed on the fully dehydrated oxide (1073 K) as evidenced by their different EPR spectrum. Surprisingly the centers formed on relatively hydroxyl rich surfaces (Figure 8b,c) do not exhibit an appreciable hyperfine interaction with protons.

Quantum Chemical Calculations. Cluster models and ab initio wave functions have been used to study the electronic structure of various types of F_s^+(H) centers. Two basic models of an oxygen vacancy containing a trapped electron were considered: (a) the vacancy is located on the (001) surface and (b) it is on the edges (001, 010) or steps of the MgO cubic microcrystal. In fact, previous work[28] has shown that the stability of the trapped electron in these two types of surface vacancies is comparable and is determined by the strong attractive potential of the ionic lattice.

In the present case the influence of a neighboring hydroxyl group on the electron spin densities of the two vacancies has been calculated at the all-electron-restricted Hartree−Fock level (RHF) using stoichiometric clusters of ions embedded in a large array of ± 2 point charges. Flexible basis sets of double-ζ quality were used for the description of the cations and anions and of the trapped electron in the vacancy (for further details see ref 28). The interacting OH group was assumed to be close to the vacancy, and the local geometrical relaxation of the ions around the vacancy was taken into account by means of analytical gradients optimization. The presence of an hydroxyl group on the cluster was represented by adding a proton, H^+, on top of a surface or edge O^{2-} ion. The optimal O−H distance, 0.95−0.96 Å depending on the site, surface or edge, was fixed in most of the calculations. The addition of a proton to model the formation of an OH group leads to a cluster which is doubly charged (formally, one positive charge is localized in the cavity and one on the H atom). This may have consequences on some of the computed properties as will be discussed more in detail below. A schematic representation of the clusters used in the calculations of the F_s^+(H) centers is reported in Figure 9 (a-1).

The spin densities and the corresponding isotropic hyperfine coupling constants (a_{iso}) for each individual center have been computed by means of unrestricted Hartree−Fock calculations (UHF); the values of $\langle S^2 \rangle = 0.75 \pm 0.02$ indicate that the states correspond to pure doublets with no spin contamination. The results based on UHF calculations of the F_s^+(H) models shown in Figure 9 are summarized in Table 2. As will be discussed in detail below, we have considered all possible locations of the proton near the oxygen vacancy on a terrace or a step. For each system we report the a_{iso} value and the spin density at nucleus for the H atom and for each of the nonequivalent Mg^{2+} ions (Table 2). This is essential in order to show with the help of Figure 9 the preferential polarization of the trapped electron toward one of these sites. All the calculations were performed with the HONDO 8.5 program[37] on IBM Risc 6000 workstations.

The dependence of the computed isotropic coupling constants on cluster size, on the coordination of the ions around the vacancy, and on basis set has been carefully checked,[38] and one can exclude a significant dependence of a_{iso} on these variables. To test the reliability of the theoretical values of the spin densities and isotropic coupling constants, a F^+ center in bulk MgO was calculated using a $[Mg_6O_{12}]^{13}$ + PC's cluster; this cluster consists of 6 Mg ions describing an octahedral cavity in bulk MgO surrounded by 12 nearest-neighbor O ions. The corresponding a_{iso} value which derives from a homogeneous distribution of the spin density over the 6 equivalent Mg^{2+} cations is 4.5 G. This value is only slightly overestimated, by about 10%, in comparison with the experimental value of 3.94 G.[3,4,39]

Despite this encouraging result, some care is necessary in comparing the theoretical with the experimental data. In fact, the isotropic coupling constants are very delicate quantities depending on a series of factors. Very little experience exists on the evaluation of these constants in ionic crystals like MgO. In particular, three effects can be of significant importance for the calculation of these observables: (a) the extent of geometrical relaxation around the vacancy, (b) electron correlation,

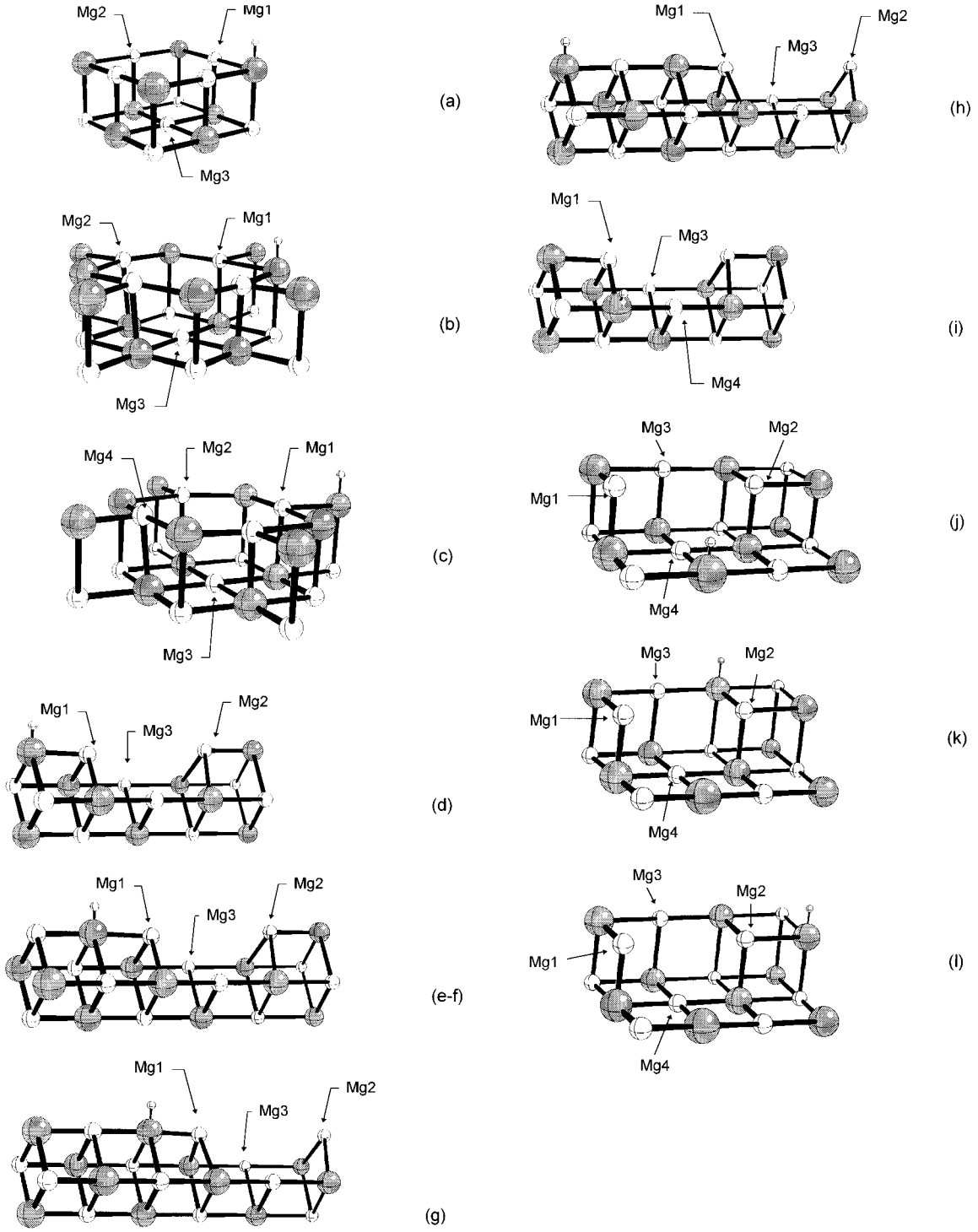

Figure 9. Cluster models of an oxygen vacancy, F_s^+(H), at the terrace (a−c), edge (d−i), and step (j−l), sites of the MgO surface. The position of the adsorbed proton to form a surface OH^- group is also indicated. The labels of the Mg ions refer to the hyperfine coupling constants given in Table 2. The clusters have been embedded in a large array of ±2 point charges (not shown).

and (c) the addition of a proton to represent the surface hydroxyl for the case of F_s^+(H) centers. We discuss here in more detail the consequences of each of these effects.

(a) With a cluster model it is possible to consider only a very local geometrical relaxation, involving the first and possibly the second nearest neighbors around the vacancy. On the other hand, charged defects result in substantial short- and long-range relaxation,[28] in particular for low-coordinated sites such as those on edges and corners. Given the high polarizability of the trapped electron, a change in geometrical relaxation may result in a change of the coupling constants. Calculations on clusters where the position of the Mg^{2+} ions around the vacancy has been varied (either taken from the ideal lattice or optimized, see cases a−c, d, and f in Figure 9 and Table 2) show a little dependence of a_{iso} on the local arrangement of the ions. The role of long-range lattice relaxation remains open, but to a first approximation we do not expect this to be a major problem in determining the coupling constants.

(b) The a_{iso} values in this work have been obtained at the Hartree−Fock level. It is likely that correlation effects will reduce the a_{iso} values. In fact, recent studies on the hyperfine coupling constants of small paramagnetic molecules have shown that the introduction of correlation effects (or the use of density functional theory) results in much smaller constants.[40,41] Preliminary calculations on the O_8Mg_9 model of a F_s^+ center have been performed at the DFT level using a nonlocal expression of the exchange-correlation potential. The results show that using the same bases set, the a_{iso} values computed at the UHF

TABLE 2: Hyperfine Coupling Constants for F_s^+(H) Centers at Terraces, Edges, and Steps of MgO (See Also Figure 9)[a]

cluster and nucleus[b,c]	a_{iso}, G	spin density at nucleus, au	cluster and nucleus[b,c]	a_{iso}, G	spin density at nucleus, au
Terrace			Step		
$O_8Mg_9^+-H^+$ (a)			$O_9Mg_{10}^+-H^+$ (j)		
H	−1.1	−0.001	H	−7.6	−0.005
Mg_1 (2)	−12.8	0.131	Mg_1 (1)	−10.5	0.107
Mg_2 (2)	−1.4	0.014	Mg_2 (1)	−8.6	0.088
Mg_3 (1)	−2.7	0.028	Mg_3 (1)	−1.1	0.011
$O_{12}Mg_{13}^+-H^+$ (b)			Mg_4 (1)	−6.9	0.070
H	−1.5	−0.001	$O_9Mg_{10}^+-H^+$ (k)		
Mg_1 (2)	−9.4	0.096	H	−1.7	−0.001
Mg_2 (2)	−2.1	0.022	Mg_1 (1)	−4.1	0.042
Mg_3 (1)	−2.5	0.025	Mg_2 (1)	−23.4	0.239
$O_{12}Mg_{13}^+-H^+$ (c)			Mg_3 (1)	−14.8	0.151
H	−0.3	0.000	Mg_4 (1)	−2.3	0.024
Mg_1 (1)	−12.8	0.131	$O_9Mg_{10}^+-H^+$ (l)		
Mg_2 (2)	−5.0	0.051	H	−0.1	−0.000
Mg_3 (1)	−2.5	0.025	Mg_1 (1)	−6.4	−0.065
Mg_4 (1)	−2.8	0.029	Mg_2 (1)	−29.1	0.298
			Mg_3 (1)	−6.7	0.069
Edge			Mg_4 (1)	−3.7	0.038
$O_9Mg_{10}^+-H^+$ (d)					
H	−0.11	0.000			
Mg_1 (1)	−31.2	0.319			
Mg_2 (1)	−1.7	0.018			
Mg_3 (2)	−6.1	0.062			
$O_{11}Mg_{12}^+-H^+$ (e)					
H	0.1	0.000			
Mg_1 (1)	−29.9	0.306			
Mg_2 (1)	−1.8	0.018			
Mg_3 (2)	−6.0	0.062			
$O_{11}Mg_{12}^+-H^+$ (f)					
H	−0.1	0.000			
Mg_1 (1)	−21.1	0.216			
Mg_2 (1)	−2.7	0.027			
Mg_3 (2)	−7.0	0.072			
$O_{11}Mg_{12}^+-H^+$ (g)					
H	−0.2	0.000			
Mg_1 (1)	−19.0	0.195			
Mg_2 (1)	−3.3	0.034			
Mg_3 (2)	−8.0	0.082			
$O_{11}Mg_{12}^+-H^+$ (h)					
H	−0.1	0.000			
Mg_1 (1)	−9.0	0.092			
Mg_2 (1)	−6.3	0.064			
Mg_3 (2)	−10.0	0.103			
$O_9Mg_{10}^+-H^+$ (i)					
H	−1.7	−0.001			
Mg_1 (1)	−26.9	0.275			
Mg_3 (1)	−15.0	0.153			
Mg_4 (1)	−3.6	0.036			

[a] For Mg only coupling constants larger than |−1| are reported. [b] The number of equivalent Mg ions is given in parentheses. [c] The labels in parentheses for each cluster refer to Figure 9. In particular the following cases can be distinguished: (a) vacancy geometry fixed as in ideal (100) surface; (b) vacancy geometry optimized, proton on 1st O^{2-} neighbor (to the vacancy); (c) vacancy geometry fixed as in free vacancy,[26] proton on second O^{2-} neighbor; (d) vacancy geometry optimized, proton on first O^2 neighbor on first layer; (e) same as (d) but four neighboring ions to OH included; (f) same as (e) but vacancy geometry as in free vacancy;[26] (g) geometry of vacancy same as (f), proton on first neighbor on first layer ($E = -3\,744.105\,02$ au); (h) geometry of vacancy same as (f) but proton on second neighbor on first layer ($E = -3\,744.177\,35$ au); (i) same as (d) but proton on first neighbor of second layer; (j) fixed geometry as on Mg(100), proton on first neighbor of second layer ($E = -3\,160.822\,16$ au); (k) same as in (j), proton on first neighbor of first layer ($E = -3\,160.852\,72$ au); (l) same as in (j), proton on second neighbor of first layer ($E = -31\,160.921\,01$ au).

level, −6.0 G, are almost identical with the DFT ones, −6.2 G.[38]

(c) The third limitation is connected to the special case of the F_s^+(H) centers and is due to the addition of a proton to model the OH group in the vicinity of the vacancy. A very important consequence of the presence of the OH group, which will be discussed below, is the strong polarization induced on the trapped electron. This leads to an increased spin density on the Mg cations closest to the OH group and in a larger value of a_{iso}. However, an overestimation of the polarizing power of the OH group will produce too large constants. If the H^+ added to the surface O is not properly screened by the surface electrons (i.e., it has a too acid character) it may induce a too strong polarization of the trapped electron. As it is known that OH and hydride groups form from the heterolytic dissociation of the H_2 molecule on low-coordinated ions of the MgO surface,[42] we considered another model where we adsorbed an H^+ on a surface O^{2-} and an H^- on a Mg^{2+} cation (see Figure 10). Of course, the real charges on the two H atoms are determined by the self-consistent nature of the wave function, but in this way a globally neutral unit (H^+ and H^-) is added to the cluster, instead of a charged one as for the case of the proton addition. The effect on the hyperfine coupling constants is large. When the H^+ and H^- ions are simultaneously present (Figure 10), the a_{iso} values are about a factor of 2 smaller than the corresponding values obtained by adding a proton. It is important to note that the H^- ion has been added on the opposite site of the OH group with respect to the vacancy so that it can

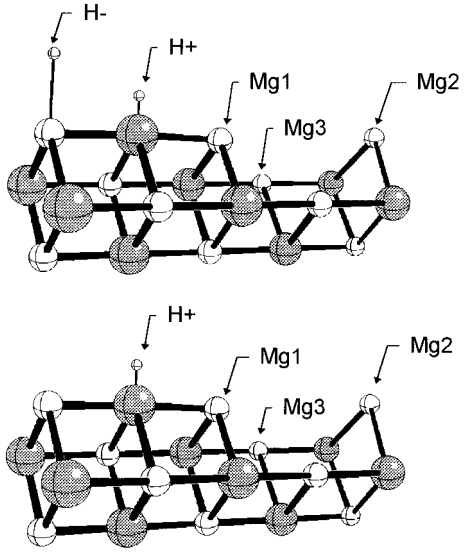

Figure 10. Cluster models of a F_s^+(H) center at an edge site where either a neutral unit, H_2, or a proton, H^+, has been added to simulate the presence of hydroxyl groups on the surface (see text).

provide only an indirect screening of the charge on the proton. This model, although very simplified, provides an indication that the polarizing power of the OH group may be exaggerated in our models.

All the intrinsic limitations in our models, in particular the absence of correlation effects and the model of the OH groups, contribute to give too high values of a_{iso}, particularly for low-symmetry sites where the trapped electron is polarized toward a single Mg^{2+} cation. For this reason, the computed coupling constants must be considered only from a qualitative point of view as a relative measure of the asymmetry induced by the OH groups on the spin distribution within the cavity. On the other hand, for high-symmetry sites such as a bulk (O_h) or a surface (C_{4v}) F_s^+ centers, we expect a much better agreement with the experiment, as shown by the similar values computed for a bulk O vacancy.

Discussion

Various methods can be used to generate surface F_s^+ centers on MgO. Irradiation of the activated MgO powder with a *suitable* dose of γ-rays (high doses produce bulk centers) causes minimum damage to the oxide lattice but populates the existing anion vacancies by ionization.[3−5] The interaction of low ionization energy metals, typically alkali and alkali-earth metals, with the oxide at a *suitable* temperature (very high temperatures produce bulk F centers) also leads to the formation of surface F_s^+ centers.[11−13,19,21,22] This interaction results in ionization of the metal atoms with subsequent stabilization of both the released electrons in the vacancies and the cations by the surface (eq 2).

$$F_s^{2+}-MgO + M^0 \rightarrow F_s^{+}-MgO + M^{+} \qquad (2)$$

On the other hand, UV irradiation of the oxide in the presence of H_2 will produce surface F_s^+(H) centers. The mechanism in this case may be described in terms of an electron transfer from the $H^\bullet$ atom (generated in the gas phase by the UV irradiation) to a surface anion vacancy (F_s^{2+}) and is thus analogous to that in eq 2. The high ionicity of the oxide is thus the driving force of the process. The surface electric field induces ionization of alkali and alkali-earth metals but also of hydrogen atoms whose ionization energy is definitely higher than that of the s-block elements. The proton resulting from $H^\bullet$ ionization is then stabilized at an O^{2-} surface ion giving rise to a surface hydroxyl group which magnetically interacts with the unpaired electron in the vacancy (eq 3).

$$H^\bullet + O^{2-}\cdots F_s^{2+}-MgO \rightarrow \underset{F_s^{+}\text{(H) center}}{OH^{-}\cdots F_s^{+}-MgO} \qquad (3)$$

Features of F_s^+(H) Derived by EPR. In the early 1970s Tench and Nelson[8] proposed a simple model for the F_s^+(H) center based on their EPR data. This model is summarized as follows:

(a) The unpaired electron is localized in a surface anion vacancy on the (001) planar face of MgO. Because of the face-centered cubic structure of the oxide, this particular vacancy has a square-pyramidal C_{4v} type symmetry. The trapped electron has therefore five neighboring Mg^{2+} cations, four of them lying in the (001) surface plane itself and the remaining cation in the apical position at the bottom of the vacancy.

(b) The trapped electron does not interact equivalently with all five cations but preferentially with one of them which is, in the proposed model, the apical Mg^{2+} cation. This preferential interaction has important effects on the EPR spectrum of the F_s^+(H) center in that it produces a weak sextet hyperfine pattern of about 10 G due to the interaction with a $^{25}Mg^{2+}$ cation ($I = {}^5/_2$). The intensity of this sextet is weak due to the relatively low natural abundance of the ^{25}Mg nuclei (10.13%). This increased spin density in the s orbital of the apical Mg^{2+} cation was explained in terms of polarization of the electron wave function toward the bottom of the vacancy.

(c) The trapped electron also interacts with a proton ($I = {}^1/_2$) belonging to a surface hydroxyl group giving the reported hyperfine splitting of about 2 G.

A graphic scheme illustrating this model was reported by Tench and Nelson.[8] However to test the validity of this model and ultimately to propose a new model, the features of the F_s^+-(H) center as derived by the above EPR and quantum chemical calculations must now be examined in detail.

^{1}H Hyperfine Tensor. The parameters, accurately derived by computer simulation, of the ^{1}H hyperfine tensor were found to be $A_{||} = 0.4$ G and $A_\perp = 2.07$ G (Table 1). The H hyperfine tensor can be decomposed into the isotropic and anisotropic parts as follows:

$$A_{exp} = a_{iso} + [B\ B - 2B] \qquad (4)$$

$$A_{exp} = [2.07\ 2.07\ 0.4] = \pm 1.51 \pm [0.56\ 0.56\ -1.12] \qquad (5)$$

The derived a_{iso} value is very small and corresponds to a percentage s character (i.e., the ^{1}H 1s character) of about 0.2%. The energy corresponding to the dipolar interaction between the electron and the proton (B) can be expressed in terms of a simple point−dipole approximation as

$$E_{dip} = B(3\cos^2\theta - 1), \quad \text{where } B = g_n\beta_n/r^3 \qquad (6)$$

In this expression g_n is the nuclear g factor, β_n the nuclear magneton, and r the electron−proton distance. Regardless of where the cation vacancy is localized (i.e., on the planar (001) face, at the (001,010) edges, on steps, etc.) the distance between the vacancy itself and the possible hydroxyl sites (the different possible O^{2-} anions bearing the interacting proton) depends on the MgO lattice parameter and on the O−H distance of the hydroxyls. On the basis of the experimental lattice parameter of MgO and adopting an OH distance of 0.96 Å, the first and second nearest hydroxyl groups are located 3.121 Å (a) and 4.308 Å (b) from the center of the vacancy respectively (see Scheme 1).

SCHEME 1

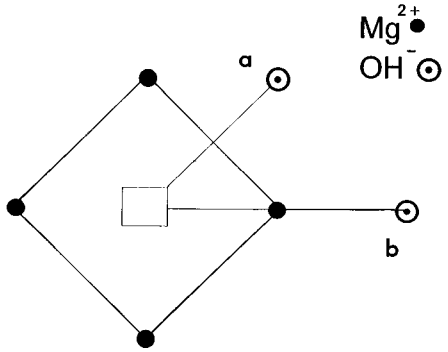

At these two given distances the estimated values of *B* (from eq 6) are 0.915 and 0.348 G, respectively. The actual experimental value for *B* (0.56 G) lies between the two calculated values. However it should be noted that the calculated B values were estimated through a crude approximation (the point dipole one). Furthermore the asymmetric distribution of the electron density in the vacancy, as evidenced by EPR and confirmed by theoretical calculations, markedly affects the *B* value. This electron distribution is not, of course, considered in the previous point−dipole calculation.

The above analysis of the hyperfine tensor unambiguously indicates that the observed EPR spectrum of the F_s^+(H) is comparable with the idea of an electron localized in a vacancy and interacting with a nearby hydroxylic proton. The same result is obtained from the theoretical calculations which show virtually no spin density on the H atom (Table 2).

^{25}Mg Hyperfine Tensor. In MgO the low abundance of the ^{25}Mg isotope seriously limits the detection of the hyperfine structure, and this problem is further compounded in the case of powder spectra due to the random orientations of the microcrystals. When the spectra are sufficiently well resolved, the magnitude of the observed hyperfine couplings provides the information on the extent of the electron interaction with the surrounding lattice cations.

Bulk F^+ color centers have been studied in single crystals of MgO by EPR[3,4,39] and an axial tensor with $a_{iso} = 3.94$ G and $B = 0.48$ G was reported. All of the six nuclei are of course equivalent. The hyperfine coupling constants can however increase remarkably if some factor which breaks the symmetry is present. This is the case of the F_c^+ center where the unpaired electron is trapped in a double cation−anion vacancy pair in the bulk of MgO.[4] The repulsive effects of the negative charges from the cationic vacancy of the F_c^+ center tends to increase the electron density on the four opposite cations surrounding the anion vacancy. An a_{iso} value of 17.5 G and $B = 0.7$ G have been reported for this center in MgO.[4]

In the case of polycrystalline MgO UV irradiated under H_2, the observations in the present work and those by Tench and Nelson[8] are in good agreement and indicate the existence of a sextet with a large ^{25}Mg coupling constant of 10−11 G (Table 1). However, a second smaller Mg hyperfine structure was observed ($a_{iso} = 0.74$ G) in the present work by carefully simulating the experimental spectrum. The two ^{25}Mg hyperfine couplings essentially suggest that the unpaired electron density in the surface defect site is inhomogeneous, and there is a preferential interaction of the trapped electron with one (or more) particular $^{25}Mg^{2+}$ cation(s). In other words the intrinsic Mg^{2+} cations surrounding the vacancy are not magnetically equivalent. The two values of $A_{||}$ and $A_{\perp}$ are rather close one to the other, indicating that the **A** tensor is nearly isotropic and that the most relevant contribution to the hyperfine structure derives from interaction with 3s orbitals of Mg^{2+}. The slightly axial character of the tensor, however, also indicates a (minor) role of 3p orbitals in this interaction.

As seen in Figure 4, the two $^{25}Mg^{2+}$ hyperfine interactions ($A(^{25}Mg)_1$ and $A(^{25}Mg)_2$) are visible only for the F_s^+(H) (or F_s^+-(D)) centers, when the neighboring OH^- group is present (Figure 4a,b). In the absence of this OH^- group, as is the case for the F_s^+ center on γ-irradiated MgO, no ^{25}Mg hyperfine interaction was visible (Figure 4c). The presence of a ^{25}Mg hyperfine structure is thus intimately related to the presence of the ^{1}H.

The complexity of the experimental spectra and the intrinsic poor resolution of a powder spectrum recorded on a high surface area heterogeneous surfaces does not allow a totally unambiguous analysis of the experimental spectra. However, the above computer simulations of the EPR spectra have demonstrated that simulation of the sextet based on the 10.13% probability that *one* single cation is ^{25}Mg, and not ^{24}Mg, does not seem to satisfactorily account for the observed intensity of the hyperfine lines. On the other hand, simulation of *two* or *three* equivalent Mg^{2+} cations, with an 18% or 24% probability that one $^{25}Mg^{2+}$ cation is present in this cation array, gives a more correct intensity of the sextet. The observed $A(^{25}Mg)_2$ sextet thus likely arises from the interaction of the electron with more than one Mg^{2+} cations. [Based on the geometrical features of the various possible sites for F_s^+(H) reported in Figure 9 it appears that in the case of 5-Mg^{2+} vacancies (Figure 9a,b) the maximum number of equivalent cations is two, whereas for the 4-Mg^{2+} sites there are no equivalent ions. As discussed before, however, the line width of the Mg hyperfine lines is quite large and a relatively high degree of inequivalency of the ions in stronger interaction with the unpaired electron could also be indistinguishable.] In conclusion the above reported spectra (Figures 1, 3, and 4) suggest that the asymmetry of the electron distribution in the vacancy depends on the influence of the OH^- group; when present (as for F_s^+(H)) there is preferential interaction with two or three Mg^{2+} cations, and when absent (as for F_s^+) there is no preferential polarization of the electron distribution to any cation. This suggestion is fully supported by the theoretical results reported in this paper which show a considerable asymmetry in the spin density for the F_s^+(H) centers.

Features of F_s^+ and F_s^+(H) Derived by Quantum Chemical Calculations. The electron distribution in surface F_s^+ centers was recently examined by theoretical calculations.[28] The electron was considered to be trapped in a vacancy at the planar face (C_{4v} symmetry with five cations surrounding the vacancy) and at the edges of the microcrystals (C_{2v} symmetry with four cations surrounding the vacancy). In the former example, for the C_{4v} symmetric case, the electron distribution in the vacancy was found to be quite homogeneous. According to the type of cluster adopted for the calculation the a_{iso} value for the apical cation varied from about 3.5 to 5.2 G, but the calculated value was always either slightly higher or slightly lower than the a_{iso} of the four equatorial cations (4.2−5.5 G). No evidence for large values like the 25 G proposed by Tench et al.[5,8] was ever found. In the case of the F_s^+ centers located at the edge positions (the C_{2v} symmetry case), the overall electron density over the four Mg^{2+} cations in the vacancy is greater compared to the F_s^+ centers located on the (001) face (essentially the same electron density is now shared among four cations instead of the five cations of the (001) face F_s centers) and ranges from 7.6 to 8.3 G for the two families of nonequivalent ^{25}Mg sites.[28]

In these two models of the surface F_s^+ centers, the electron distribution in the vacancy appears to be quite homogeneous and evenly dispersed over the four or five surrounding Mg^{2+} cations.[28] When models of a step site are considered (C_s symmetry) constants ranging from 5 to 13 G are computed;[38]

the larger values are in correspondence of the two equivalent three-coordinated Mg^{2+} cations at the corners of the vacancy. Therefore, there is a tendency toward an increase of the a_{iso} values as the symmetry of the site is reduced because the unpaired electron is inhomogeneously distributed over the *n* cations around the vacancy.

This tendency becomes even more dramatic when a model of an F_s^+(H) is considered. On a terrace, five-coordinated vacancy, the presence of the OH group breaks the symmetry which is reduced to C_s; therefore, there are at most two equivalent Mg^{2+} cations in these sites (see models a or b, Figure 9). The trapped electron is polarized toward the OH group because of the partial positive charge on the terminal H atom, and coupling constants of 10−13 G are measured, depending on the model. These constants are about twice as large as for the corresponding F_s^+ centers. When the OH group is adjacent to a Mg^{2+} ion (see case c) this is the ion which exhibits the largest coupling constant (Table 2).

On edge sites, the presence of an OH group reduces the symmetry to C_s, and very large values of a_{iso} are computed. When the OH group is nearest neighbor to the vacancy (see sites d−g and i in Figure 9), a_{iso} is between 19 and 31 G (Table 2). When the OH group is four lattice constants from the vacancy (site h), a_{iso} is reduced to 9−10 G. The largest spin density, however, is always found in correspondence to a single Mg^{2+} ion closest to the OH group. We have considered also models of F_s^+(H) centers at step sites (see cases j−l in Figure 9. Case j has a C_s symmetry, and resembles to some extent a surface F_s^+ center where one Mg^{2+} cation is replaced by an H^+ ion; however, the large value of the H coupling constant, 7.6 G, not observed experimentally, rules out this structure. In the remaining two models, k and l, there is no symmetry at all. The electron feels the attractive potential of the proton and is polarized preferentially toward the closest three-coordinated Mg^{2+} ion which exhibits coupling constants of 23−29 G.

As we discussed previously, any attempt to correlate the absolute values of the computed a_{iso} constants with the experimental values must be done with great care. However, the calculations show a very clear tendency toward a pronounced polarization of the unpaired electron toward one or two Mg^{2+} cations induced by the OH groups. If, for symmetry reasons, there is only one nonequivalent Mg^{2+} cation close to the OH group, this shows a large spin density at the nucleus and an a_{iso} value about 2−3 times larger than that on the corresponding F_s^+ center. The effect is more pronounced for the edge and the step sites because the low coordination results in a higher polarizability of the trapped electron compared to a surface site.

With this in mind, in the following section we discuss the problem of the structure and location of the F_s^+(H) centers.

Structure and Location of the F_s^+(H) Center. The combined ab initio and experimental results evidence the important role played by the OH^- group in influencing the electron distribution in the vacancy. As to the structure and location of the centers this approach allows the following considerations.

(a) As also indicated by theoretical calculations[28] the unpaired electron may be in principle trapped at either the five Mg^{2+} or four Mg^{2+} available vacancies. The simulation of the Mg hyperfine structure does not remove such uncertainty because the differences of the profiles obtained by considering a four Mg^2 vacancy are not really distinguishable from those of vacancies with five Mg^{2+} cations. The calculated values of a_{iso} for the five Mg^{2+} case are, however, in closer agreement with the experimental values than those for the four Mg^{2+} case which are higher. Moreover, as discussed before, in the case of the five cations site the location of the OH group illustrated in Figure 9a,b determines the equivalency of two Mg ions.

(b) The formation of oxygen vacancies at the MgO surface has been related to the process of surface dehydration. This latter process is believed to be a non random process and to follow a quite regular pathway as shown by IR studies.[29,30] The first step involves the dehydration of the planar faces and is followed by dehydration of the edges and corner sites where low coordination cations and anions are present ($Mg^{2+}_{4c,3c}O^{2-}_{4c,3c}$). Coluccia et al.[29] have proposed that the formation of surface oxygen vacancies accompanies the last part of the dehydration process when few OH^- ions are left at the surface mainly at these particular low-coordination surface sites. On the basis of this dehydration model, therefore, O^{2-} vacancies should be more probably found at edges of the microcrystals and similar locations rather than at planar (001) faces where the energy needed to extract a 5C O^{2-} anion is higher than that needed for the same ion with lower coordination. On the basis of the described model, the observed F_s^+(H) centers should thus be preferentially located at the edges of microcrystals where low coordination ions are found. This indication contrasts with those reported at point (a) suggesting a five Mg^{2+} vacancy.

The accepted model of surface dehydration, however, should be reexamined since the process is likely more complex than that previously reported.[29,30] This is demonstrated by the experiment in Figure 8 which has definitely shown that the partially dehydrated surfaces contain a relevant amount of defect sites capable of hosting electrons. This is in contrast with the idea of surface vacancies formed exclusively in the very final step of dehydration.[28,30] The F_s^+(H) centers (Figures 1 and 8a) are, however, definitely different from those formed on partially hydrated MgO (Figure 8b,c). It can therefore be concluded that although some uncertainty remains about the location of F_s^+-(H) centers, the present work indicates that they are intimately related to those particular vacancies formed in the final part of dehydration. The whole dehydration process involves the transient formation of other types of electron trapping vacancies which, at outgassing temperature higher than 873 K, evolute toward the final form.

Summarizing, a model of a vacancy containing five Mg^{2+} two of which are equivalent with respect to a nearby hydroxyl group represents the best fit between experimental results and theoretical calculation. The presence of four Mg^{2+} centers with polarization of the electron density toward three not strictly equivalent cations close to the OH group (Figure 9) cannot be, however, completely ruled out.

Nature of Centers C and D. The remaining centers which are formed on UV-irradiated MgO are centers B and C (Table 1). The low intensity of both signals and the overlap between signal B and signal A hamper a detailed investigation on the nature of these centers. The whole shape of signal B is not directly observed on the experimental spectrum but indirect information derives from Figure 7 which reports the profile of signal B derived from simulation. The similarity of this profile with that of the F centers on partially hydrated systems (Figure 8) is evident even though the assignment of these two signals to the same center is premature.

Center C was previously observed by some of us[13] and assigned to an F^+ color center localized in the bulk or, more precisely, in the immediate subsurface layers of the oxide. This idea was suggested by the symmetric nature and the *g* values of the signal, both of which are very close to those expected for bulk F^+ centers in MgO.

As for the main center observed on γ-irradiated samples (Table 1), it should be remembered that center D was formed on the same type of MgO samples as those used for UV

irradiation (T_{dehy} = 1073 K), except that the activated oxide was γ-irradiated in the absence of hydrogen. It can thus be inferred that the unpaired electron is localized in the same type of vacancy of the F_s^+(H) species but without the interaction from the nearby OH^- group. However the absence of a visible ^{25}Mg hyperfine structure in the EPR of center D is not, at present, understood unless if the spin density on each ion of the vacancy were, for unknown reasons, extremely low. The analysis of this signal is beyond the scope of the present paper, and the problem is currently under investigation in our laboratories also by means of ENDOR spectroscopy.

Conclusions

F_s^+(H) centers are paramagnetic surface centers formed on MgO by UV irradiation of the activated oxide under a hydrogen atmosphere. In the present work the structure and location of this surface color center on MgO has been redefined using a combined EPR and quantum chemical approach. The center can be described as an excess electron trapped in a surface anion vacancy. A dipolar interaction occurs between this trapped electron and the proton from a neighboring surface OH^- group. The electron distribution in the vacancy is inhomogeneously dispersed over the constituent Mg^{2+} cations due to the preferential polarization of the electron wave function toward the Mg^{2+} cations closest to this OH^- group. This preferential spin polarization over two or more cations, with the resulting smaller spin density on the remaining cations in the vacancy, was directly evidenced by EPR (the $A(^{25}Mg)_1$ and $A(^{25}Mg)_2$ hyperfines), interpreted by EPR simulations, and confirmed by theoretical calculations. The exact number of cations surrounding the vacancy cannot be unambiguously established on the basis of the present data even though the indication from quantum chemical calculations are in favour of a five Mg^{2+} vacancy with two magnetically equivalent cations (Figure 9a,b). We have demonstrated that the F_s^+(H) centers do not form on partially hydrated samples (where different and previously unreported centers are formed) but are typical of thoroughly dehydrated materials. These findings, which appear in contrast with the current models of surface dehydration, will probably stimulate further research on the problem of surface defect formation on oxide surfaces. The mechanism proposed for F_s^+-(H) center formation (eq 3) emphasizes the role of the ionizing properties of MgO surface which induce the ionization of the atoms produced in the gas phase by UV irradiation in strict analogy with the process occurring upon contact between MgO and alkali-metal atoms.

References and Notes

(1) Hutchinson, C. A. *Phys. Rev.* **1949**, *75*, 1769.
(2) Weber, H. *Z. Phys.* **1951**, *130*, 392.
(3) Wertz, J. E.; Orton, J. W.; Auzins, P. *Discuss. Faraday Soc.* **1961**, *30*, 40.
(4) Henderson, B.; Wertz, J. E. *Adv. Phys.* **1968**, *17*, 749.
(5) Nelson, R. L.; Tench, A. J.; Harmsworth, B. J. *Trans. Faraday Soc.* **1967**, *63*, 1427.
(6) Tench, A. J.; Nelson, R. L. *Trans. Faraday Soc.* **1967**, *63*, 2254.
(7) Nelson, R. L.; Tench, A. J. *Trans. Faraday Soc.* **1967**, *63*, 3039.
(8) Tench, A. J.; Nelson, R. L. *J. Colloid Interface Sci.* **1968**, *26*, 364.
(9) Nelson, R. L.; Harmsworth, B. J.; Tench, A. J. *Trans. Faraday Soc.* **1968**, *64*, 2521.
(10) Tench, A. J. *Surf. Sci.* **1971**, *25*, 625.
(11) Zecchina, A.; Scarano, D.; Marchese, L.; Coluccia, S.; Giamello, E. *Surf. Sci.* **1988**, *194*, 513.
(12) Giamello, E.; Ferrero, A.; Coluccia, S.; Zecchina, A. *J. Phys. Chem.* **1991**, *95*, 9385.
(13) Giamello, E.; Murphy, D.; Ravera, L.; Coluccia, S.; Zecchina, A. *J. Chem. Soc., Faraday Trans.* **1994**, *90*, 3167.
(14) Tench, A. J.; Holroyd, P. *Chem. Commun.* **1968**, 471.
(15) Lunsford, J. H.; Jayne, J. P. *J. Phys. Chem.* **1966**, *44*, 1487.
(16) Che, M.; Tench, A. J. *Adv. Catal.* **1983**, *32*, 1.
(17) Giamello, E.; Murphy, D.; Garrone, E.; Zecchina, A. *Spectrochim. Acta* **1993**, *49A*, 1323.
(18) Giamello, E.; Murphy, D.; Marchese, L.; Marta, G.; Zecchina, A. *J. Chem. Soc., Faraday Trans.* **1993**, *89*, 3715.
(19) Giamello, E.; Murphy, D. In *Radicals on Surfaces*; Lund, A., Rhodes, C., Eds.; Kluwer Academic Publications: Dordrecht, 1995; Vol. 13, p 147.
(20) Smith, D. R.; Tench, A. J. *Chem. Commun.* **1968**, 1113.
(21) Murphy, D.; Giamello, E. *J. Phys. Chem.* **1995**, *99*, 15172.
(22) Kijenski, J.; Malinowski, S. *J. Chem. Soc., Faraday Trans 1* **1978**, *74*, 230.
(23) Colburn, E. A. *Surf. Sci. Rep.* **1992**, *15*, 281.
(24) Pisani, C.; Dovesi, R.; Roetti, C. *Hartree-Fock Ab Initio Treatment of Crystalline Systems*; Springer: Berlin, 1988; Lecture Note in Chemistry, Vol 48.
(25) Causà, M.; Dovesi, R.; Pisani, C.; Roetti, C. *Acta Crystallogr.* **1986**, *B42*, 247; *Surf. Sci.* **1986**, *175*, 551.
(26) Nygren, M. A.; Pettersson, L. G. M.; Barandiaran, Z.; Seijo, L. *J. Chem. Phys.* **1994**, *100*, 2010.
(27) Pacchioni, G.; Sousa, C.; Illas, F.; Parmigiani, F.; Bagus, P. S. *Phys. Rev. B* **1993**, *48*, 11573.
(28) Ferrari, A. M.; Pacchioni, G. *J. Phys. Chem.* **1995**, *99*, 17010.
(29) Coluccia, S.; Lavagnino, S.; Marchese, L. *Mater. Chem. Phys.* **1988**, *18*, 445.
(30) Coluccia, S.; Marchese, L. *Proc. Int. Symp. Acid-Base Catal.* **1988**, 207.
(31) Coluccia, S. In *Adsorption and Catalysis on Oxide Surfaces*; Che, M., Bond, G. C., Eds.; Studies in Surface Science and Catalysis; Elsevier: Amsterdam, 1985; Vol. 21, p 59.
(32) Coluccia, S.; Baricco, M.; Marchese, L.; Martra, G.; Zecchina, A. *Spectrochim. Acta* **1993**, *49A*, 1289.
(33) Zecchina, A.; Stone, F. S. *J. Chem. Soc., Faraday Trans. 1* **1976**, *72*, 2364.
(34) Garrone, E.; Zecchina, A.; Stone, F. S. *Philos. Mag., B* **1980**, *42*, 683.
(35) Mabbs, F. E.; Collison, D. *Electron Paramagnetic Resonance of d transition metal compounds*; Elsevier: Amsterdam, 1992; Chapter 7 and references therein.
(36) Pacchioni, G.; Ferrari, A. M.; Giamello, E. *Chem. Phys. Lett.* **1996**, *255*, 58.
(37) Dupuis, M.; Johnston, F.; Marquez, A. *HONDO 8,5 for CHEM-station*, IBM Corp., Kingston, 1994.
(38) Ferrari, A. M.; Pacchioni, G., to be published.
(39) Wertz, J. E.; Auzins, P.; Weeks, R. A.; Silbee, R. H. *Phys. Rev.* **1957**, *107*, 1535.
(40) Barone, V. *J. Chem. Phys.* **1994**, *101*, 6834.
(41) Chipman, D. M. *Theor. Chim. Acta* **1992**, *82*, 93.
(42) Coluccia, S.; Boccuzzi, F.; Ghiotti, G.; Morterra, C. *J. Chem. Soc., Faraday Trans. 1* **1982**, *78*, 2111.